Eur Radiol (2013) 23:3466–3476
DOI 10.1007/s00330-013-2968-x

ONCOLOGY

Whole-body diffusion-weighted imaging: is it all we need for detecting metastases in melanoma patients?

Giuseppe Petralia · Anwar Padhani · Paul Summers · Sarah Alessi · Sara Raimondi · Alessandro Testori · Massimo Bellomi

Received: 18 February 2013 / Revised: 30 May 2013 / Accepted: 22 June 2013 / Published online: 25 July 2013

Abstract
Objectives To investigate whether whole-body diffusion-weighted imaging (WB-DWI) alone is adequate for detecting metastases in melanoma patients, or if standard WB contrast-enhanced magnetic resonance imaging (WB-ceMRI) is required.
Methods Seventy-one WB-DWI studies were performed quarterly along with whole-body MRI including contrast-enhanced sequences (WB-ceMRI) in 19 patients with advanced melanoma. The reference standard was biopsy, other imaging investigations, or changes observed on follow-up. Findings of metastasis in separate WB-DWI and WB-DWI + WB-ceMRI readings were compared using κ statistics. Additionally, the distribution of findings was examined and calculated per body region (brain, neck, chest, abdomen, liver, pelvis, subcutaneous tissues, bones) and diagnostic accuracy (DA), sensitivity, specificity, negative predictive value, and positive predictive value were calculated per patient.
Results The eight examinations that were positive by the reference standard contained a total of 14 metastatic findings. With almost perfect agreement between techniques (κ=85 %, 95 % CI 70–100 %) for detection of examinations with metastatic findings, and complete agreement in extracranial metastasis detection, 10 metastases were detected using WB-DWI and 13 using WB-DWI + WB-ceMRI. WB-DWI and WB-DWI + WB-MRI had equivalent per patient DA (79 %).
Conclusions WB-DWI without additional WB-ceMRI sequences is promising for the detection of extracranial metastases in melanoma patients, but contrast-enhanced MRI is required for evaluating the brain.
Key Points
- *Whole-body (WB) magnetic resonance imaging (MRI) is increasingly used for oncological disease assessment.*
- *WB diffusion-weighted MRI detects extracranial metastases in melanoma patients.*
- *Contrast-enhanced MRI is only required for detecting brain metastases.*
- *WB-DWI is inferior to low-dose CT for detecting lung metastases.*

Keywords Whole-body imaging · Diffusion-weighted MRI · Melanoma · Metastasis · Contrast-enhanced MRI

Abbreviations and acronyms

ADC	apparent diffusion coefficient
MIP	maximum intensity projections
MPR	multi-planar reformatted images

Electronic supplementary material The online version of this article (doi:10.1007/s00330-013-2968-x) contains supplementary material, which is available to authorized users.

G. Petralia (✉) · P. Summers · S. Alessi · M. Bellomi
Department of Radiology, European Institute of Oncology,
Via Ripamonti 435, 20141 Milan, Italy
e-mail: giuseppe.petralia@ieo.it

A. Padhani
Paul Strickland Scanner Centre, Mount Vernon Cancer Centre,
Rickmansworth Road, Northwood, Middlesex
HA6 2RN, England, UK

S. Raimondi
Division of Epidemiology and Biostatistics,
European Institute of Oncology,
Via Ripamonti 435, 20141 Milan, Italy

S. Raimondi
Dipartimento di Medicina del Lavoro
"Clinica del Lavoro Luigi Devoto", Sezione di Statistica Medica e Biometria "GA Maccacaro", University of Milan, Milan, Italy

A. Testori
Melanoma and Soft Tissue Sarcoma Surgery Division,
European Institute of Oncology,
Via Ripamonti 435, 20141 Milan, Italy

M. Bellomi
School of Medicine, University of Milan, Milan, Italy

WB-ceMRI whole-body magnetic resonance imaging
WB-DWI whole-body diffusion-weighted imaging

Introduction

Although only about 1 % of all cancer deaths are attributed to melanoma, in recent decades the incidence of this disease has grown steadily in both sexes in almost all countries [1]. It is estimated that 76,690 new cases of melanoma will be diagnosed and 9,480 deaths from melanoma will be reported in the USA in 2013 [2]. The American Joint Committee on Cancer (AJCC) classifies melanoma into four stages. Stage III (any thickness melanoma tumour with involvement of regional lymph nodes and/or in-transit metastases) and stage IV (presence of distant metastases) disease are considered as advanced, with 5-year survival between 46 and 69 % for stage III and between 18 and 62 % for stage IV [3].

Surgery remains the most effective treatment for melanoma even in advanced stages, because it improves the prognosis of patients with metastases [4, 5]. Surgery is most effective when performed early in the course of disease [6, 7]. As both timing and sites of melanoma dissemination are unpredictable, it would be extremely useful to have a whole-body imaging technique for the periodic follow-up of patients with advanced melanoma. This would enable metastases to be detected early, thereby making surgery both possible and less mutilating, with the aim not only of improving patient survival but also of preserving the quality of life. At present, however, diagnostic approaches tend to vary from centre to centre as there is an absence of consensus guidelines for the follow-up of patients with advanced melanoma.

Computed tomography (CT) and fluorodeoxyglucose positron emission tomography (PET) are often used in clinical practice because they have provided good performance and availability [8, 9]. However, owing to the serial nature of follow-up imaging, a strategy based on non-ionizing radiation is highly desirable. Ultrasound is useful in the evaluation of the primary tumour and regional lymph nodes [10], but is ill-suited to whole-body evaluations for the detection of distant metastases, with a resultant poor sensitivity (approximately 53 %, compared to 85 % for CT) [11]. Magnetic resonance imaging (MRI) has shown encouraging results for detecting metastases in melanoma patients, with performance comparable to those of CT and PET/CT [12–17]. Whole-body MRI (WB-ceMRI) using T1- and T2-weighted sequences (with or without contrast injection) still sees limited use in clinical routine because it is technically challenging, involves long examinations that make it demanding on the patients, and the protocols are not yet validated against established techniques.

There is growing evidence that whole-body diffusion-weighted imaging (WB-DWI) is effective in metastases detection, with encouraging results having been shown in different tumour types [18–20]. WB-DWI has the advantages over WB-ceMRI of a relatively short acquisition, and straightforward interpretation. An open question is whether, in the surveillance of patients at high risk of developing metastases, such as those with advanced melanoma, WB-DWI and WB-ceMRI provide a cumulative benefit as part of a metastasis detection protocol. Thus, the purpose of this study was to investigate whether WB-DWI alone is adequate for detecting metastases in melanoma patients, or if standard WB-ceMRI is required.

Materials and methods

Patients

All patients signed informed consent before enrolment into this study that was approved by the institutional ethics committee. Between February 2009 and May 2011, 71 WB-DWI and WB-ceMRI studies were performed in the same session in 19 patients (mean age ± SD at first scan, 58±13.8 years; 7 female) with stage III melanoma before treatment (baseline) and every 3 months until disease progression. The follow-up in our cohort was between 3 and 27 months (median, 9 months).

All patients were part of a randomized double-blind phase III multicentre study with the objective of evaluating the role of adjuvant immunotherapy with monoclonal anti-cytotoxic T-lymphocyte antigen 4 (anti-CTLA-4) antibody (ipilimumab, Bristol-Myers Squibb, New York , USA) compared to placebo after radical surgery in patients with stage III melanoma. Inclusion criteria were histologically confirmed melanoma excised within 90 days before the baseline MRI, a diagnosis of stage III melanoma according to AJCC criteria [3], the absence of contraindications to MRI or the administration of paramagnetic contrast agent, and the absence of residual disease after surgery. Exclusion criteria were marked renal impairment (glomerular filtration rate <30 mL/min), a history of other cancer in the 5 years preceding the diagnosis of melanoma, or extra-nodal stage III disease (e.g. in-transit metastases). The appearance of distant metastases with subsequent transition to stage IV was an exit criterion of the study, following which patients underwent alternative treatments. The trial allowed for post-surgical monitoring by either CT or MRI (with low-dose chest CT), with the modality remaining the same for the duration of a patient's participation in the trial. Those patients opting for MRI-based surveillance formed the population for the present study.

Imaging technique

The protocol included WB-DWI and WB-ceMRI (including a state-of-the-art MR imaging from head to pelvis and contrast-enhanced sequences) performed at 1.5 T (Magnetom Avanto, Siemens Healthcare Sector, Erlangen, Germany), as summarized in Tables 1, 2 and 3. Before the

Table 1 MR pulse sequence parameters for WB-DWI

Scanning parameters (1.5 T)	WB-DWI
Image contrast	DWI
Imaging sequence	SSH SE EPI
Orientation	Axial
Echo/repetition time (ms)	72/6,600
Field of view (mm)	360×400
Matrix	130×160
Slices per station/stations	40/4
Slice thickness/gap (mm)	6/0
Number of signal averages	4
Flip angle (°)	90
Fat suppression	SPAIR
Respiratory control	Free-breathing
Parallel imaging factor[a]	2
Diffusion encoding	
b values (s/mm^2)	0, 800
Gradient pattern	3-scan trace
Acquisition time per station (min:s)	2:05

SSH SE EPI single-shot spin echo echo planar imaging, *SPAIR* spectral adiabatic inversion recovery

[a] Where applied, the GRAPPA (GeneRalized Autocalibrating Partially Parallel Acquisition) algorithm was used

availability of moving table acquisitions across anatomical stations, a multi-station version of the T1- and T2- weighted TSE sequences was used which provided equivalent coverage, and spatial resolution, but required additional MR machine time for repositioning. Of the 71 examinations performed, 37 made use of the moving table and 34 the multi-station acquisitions. This protocol made use of anatomy-specific phased-array surface coils for all body regions. A hepatobiliary-specific contrast agent (Gd-EOB-DTPA, Bayer-Schering, Berlin, Germany) was used, administered at a dose of 0.025 mmol/kg body weight, via an automatic injector at a flow rate of 1.5 mL/s, followed by a normal saline solution bolus (20 mL) at the same flow rate. The cumulative MR data acquisition time was 38 min 21 s, including 8 min 20 s for WB-DWI, and 30 min 1 s for WB-ceMRI, making for a total examination time of around 55 min (see "Results").

Image analysis

The images were processed on a dedicated workstation (Leonardo, Siemens Healthcare Sector, Erlangen, Germany) to produce a unified axial series covering from head to pelvis consisting of DW images with $b=800$ s/mm^2, and of greyscale apparent diffusion coefficient (ADC) maps. A composite sagittal T1 series covering the entire spine was likewise generated. Maximum intensity projections (MIPs) around the cranio-caudal axis (120 projections, 3° separation) and multi-planar reformatted images (MPRs) in the coronal plane (5/0 mm thickness/gap) were reconstructed from the unified DW axial series with $b=800$ s/mm^2 and displayed in inverted greyscale.

Table 2 MR pulse sequence parameters for post-contrast WB-MRI scans

Scanning parameters (1.5 T)	WB-T1	Head & neck	Abdomen	Spine[d]
Image contrast	T1 Dixon[c]	T1	T1	T1
Imaging sequence	FLASH	Spin echo	VIB	TSE
Orientation	Axial	Axial	Axial	Sagittal
Echo/repetition time (ms)	2.38, 4.764/124	9.7/501	1.75/4.88	11/395
Field of view (mm)	287.5×400	272×320	287.5×400	380×380
Matrix	179×320	190×320	161×320	224×448
Slices per station/stations	14/13	50/1	60/1	18/2
Slice thickness/gap (mm)	5/1	5/1	4/0	3.5/0.4
Number of signal averages	1	1	1	2
Flip angle[a] (°)	90	90	10	150
Fat suppression	–	–	SPAIR	–
Respiratory control	Breath-hold	–	–	–
Parallel imaging factor [b]	2	–	2	2
Acquisition time per station (min:s)	1:42	4:53	0:19	3:58

FLASH fast low-angle shot, *VIBE* volume interpolated breath-hold examination (gradient echo), *SPAIR* spectral adiabatic inversion recovery

[a] For TSE sequences, refocusing angle is given

[b] Where applied, the GRAPPA (GeneRalized Autocalibrating Partially Parallel Acquisition) algorithm was used

[c] With "water" and "fat" image reconstruction

[d] Sequence repeated for cervical, thoracic and lumbar spine

Table 3 Parameters used for post-contrast WB-ceMRI scans

Scanning parameters (1.5 T)	WB-T1	WB-T2	Head & neck			Abdomen	
Image contrast	T1 Dixon[c]	T2[d]	T1	T1	T2[c]	Dynamic & late phase T1	T2
Imaging sequence	FLASH	BLADE TSE	SE	SE	TSE	VIBE	HASTE
Orientation	Axial	Axial	Axial	Coronal	Axial	Axial	Axial
Echo/repetition time (ms)	2.38, 4.764/124	210/2,660	9.7/501	8.4/489	128/3,610	1.75/4.88	117/1,300
Field of view (mm)	287.5×400	400×400	272×320	195.5×230	270×320	287.5×400	256×320
Matrix	179×320	256×210	190×320	190×320	227×384	161×320	230×320
Slices per station/stations	14/13	128/1	50/1	24/1	50/1	60/1	30
Slice thickness/gap (mm)	5/1	5/1	5/1	5/1	5/1	4/0	6/1.2
Number of signal averages	1	1	1	1	2	1	1
Flip angle[a] (°)	90	130	90	90	150	10	150
Fat suppression	–	–	–	–	–	SPAIR	–
Respiratory control	Breath-hold	Breath-hold	–	–	–	–	Breath-hold
Parallel imaging factor[b]	2	2	–	–	2	2	2
Acquisition time per station (min:s)	1:42	2:40	4:53	3 : 12	2: 42	0:57 (dynamic) 0:19 (late phase)	0:39

FLASH fast low-angle shot, *VIBE* volume interpolated breath-hold examination (gradient echo), *SSH SE EPI* single-shot spin echo echo planar imaging, *SPAIR* spectral adiabatic inversion recovery

[a] For TSE sequences, refocusing angle is given

[b] Where applied, the GRAPPA (GeneRalized Autocalibrating Partially Parallel Acquisition) algorithm was used

[c] With "water" and "fat" image reconstruction

[d] All T2-weighted images and the upper abdomen DWI were acquired after contrast administration and dynamic T1 scan of the abdomen to make use of the time available prior to performing the hepatobilary "late" phase T1 scan (ca. 20 min)

Each MR examination was prospectively analysed by one of four radiologists who had between 5 and 14 years of experience in oncologic MRI. Two radiologists (randomly chosen from the pool of four) each prospectively and separately read one of WB-DWI and WB-DWI + WB-ceMRI for a given patient exam. Each radiologist reported the presence of a finding when one or more lesions were detected in any of seven body regions (brain, neck, chest, abdomen, pelvis, subcutaneous tissues and bones), measured their size (or in the presence of multiple lesions, their minimum and maximum sizes), and categorized them as either benign or suspicious/diagnostic for malignancy. The readers recorded their findings for the study. Any clinical decisions were based on consensus of the two readers.

The evaluation of the examinations was based on morphological characteristics, enhancement pattern, and DWI appearance. General radiological criteria for metastases were areas with shape suggestive of tumour, abnormal signal and/or pathological enhancement after intravenous contrast agent injection, and hyperintense appearance on DWI with b=800 s/mm^2 and corresponding low apparent diffusion coefficient (ADC) values. A lymph node was rated as suspicious if its largest diameter was greater than 10 mm and its appearance was round (as opposed to oval). Lymph nodes smaller than 10 mm, but hyperintense on T1 sequences (suggestive of the presence of melanin), were also rated as suspicious [12].

Subcutaneous tissue findings were considered apart as a single body region irrespective of location, and not included in body region of origin in subsequent statistical analysis. The readers recorded their findings for the study. Any clinical decisions were based on consensus of the two readers.

Reference standard

For lung assessment, all patients underwent low-dose chest CT performed using 16-slice multidetector CT (GE Lightspeed, General Electric Healthcare, Milwaukee, WI, USA) at each visit. The exposure at a single visit was 1 mSv (CT parameters in Table 4), with an estimated annual radiation dose of 4 mSv (low-dose CT was performed quarterly, at 3-month intervals).

Lesions suspicious for malignancy on WB-DWI, or WB-DWI + WB-ceMRI, that were accessible for ultrasound-guided biopsy, underwent second-look ultrasound and, in case of persistence of suspicion, needle biopsy under ultrasound guidance. Any lesion that was not accessible for ultrasound-guided biopsy or that was too small to be subjected to needle biopsy was referred for assessment on other imaging modalities, or for monitoring of changes in

Table 4 Acquisition parameters for low-dose thoracic CT

CT parameter	Value
Tube current (mAs)	30–50
Tube voltage (kV)	100–120
Gantry rotation interval (s)	0.75
Field of view (mm)	400
Acquired slice thickness (mm)	2.5
Reconstructed slice thickness (mm)	1.25
Equivalent dose (mSv)	1

subsequent study examinations. If the size increased, they were then considered malignant, whereas those whose size was stable or decreased were considered benign.

In cases considered suspicious/diagnostic for malignancy, malignancy was confirmed by histology or progression on follow-up. All the remaining findings were considered benign unless progression was observed at follow-up.

Statistical analysis

All findings reported on a first reading (using WB-DWI) and on a second reading using (WB-DWI + WB-ceMRI) were included in the statistical analysis according to their classification as benign or suspicious/diagnostic for malignancy. For these two sets of readings, we separately defined true positives (TP) as those findings classified as suspicious for malignancy that were found to be malignant by the described reference standard; true negative (TN) as benign findings that were confirmed by the reference standard; false positive (FP) as findings that were suspicious for malignancy but then proved to be benign; and false negative (FN) as findings that were considered benign but then proved to be malignant.

The agreement between WB-DWI and WB-DWI + WB-ceMRI in detecting examinations with any metastasis was calculated using κ statistics, with 95 % confidence interval (CI).

The sensitivity (SE) of WB-DWI and WB-DWI + WB-ceMRI in the detection of metastatic findings, and their positive predictive value (PPV) were calculated using the reference standard described above. McNemar's test was used to assess any significant difference in the detection of metastasis with the two different protocols (WB-DWI and WB-DWI + WB-ceMRI).

As further secondary analyses, we examined the distribution of reported findings per body region and metastases detection performance per patient. Because of the small numbers of findings per body region, a statistical breakdown by body region was excluded. For each per patient analysis, the diagnostic accuracy (DA) of WB-DWI and WB-DWI + WB-ceMRI, defined as the ratio between the sum of TP and TN and total number of patients having reported lesions, was also calculated. We further calculated the sensitivity (SE), specificity (SP), the negative predictive value (NPV) and the positive predictive value (PPV) of WB-DWI and of WB-DWI + WB-ceMRI for the diagnosis of malignancy per patient. Confidence intervals (CIs) for these values were calculated on the basis of a binomial distribution. In this secondary per patient analysis precedence was given to FN findings where multiple findings were present for a patient, as opposed to TP findings in the per examination analysis.

Results

The average overall duration of the WB-DWI + WB-ceMRI protocol was 55 min (range 53–72 min) from the start of the examination to patient discharge, with the time in excess of the 38 min 21 s dedicated to MR data acquisition occupied by patient positioning, shimming, patient instruction, localiser imaging, table movement, etc. All examinations were successfully completed, with no MR examinations considered unreadable due to motion artefacts, and there were no adverse reactions to injected contrast medium. Twelve of the 71 examinations performed (16.9 %) led to suspicious findings requiring further investigation (five second-look ultrasounds, six second-look ultrasounds with ultrasound-guided needle biopsy, and one MRI of the pituitary gland), of which 3 (25 %) showed the presence of metastases (Fig. 1a–c).

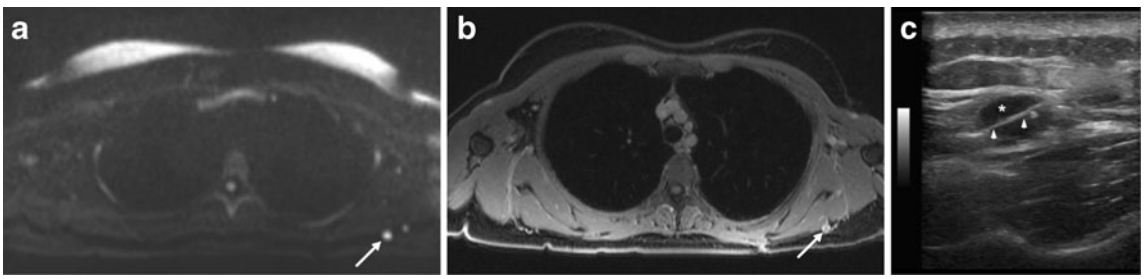

Fig. 1 A lesion of 7 mm in subcutaneous tissues in a 44-year-old woman seen as **a** a hyperintense lesion (*arrow*) on axial WB-DWI images (b=800 s/mm^2) that **b** showed enhancement (*arrow*) in post-contrast T1-weighted gradient echo "water" images. **c** The lesion (*asterisk*), located in the subcutaneous fat of the left scapular region, was considered suspicious for malignancy both using WB-DWI and WB-DWI + WB-ceMRI, and therefore the patient underwent ultrasound-guided biopsy that was positive for malignancy (the 18-gauge biopsy needle indicated by *arrowheads*)

Per examination analysis

Seventy-one examinations were performed in 19 patients. According to our standard of reference, there was at least one metastatic finding in eight examinations (Supplementary Table 1). WB-DWI revealed the presence of at least one metastatic finding in 11 examinations (15 %), whereas WB-DWI + WB-ceMRI did so in 14 examinations (20 %). Both WB-DWI and WB-DWI + WB-ceMRI correctly identified the eight positive examinations that were positive by the reference standard. The agreement of the two protocols in detecting examinations with at least one metastatic finding was almost perfect: κ=85 % (95 % CI 70–100 %).

In the eight examinations that were positive by the reference standard, there were a total of 14 metastatic findings. Of these, 10 were detected using WB-DWI (10 TP, 4 FN findings), whereas 13 were detected using WB-DWI + WB-ceMRI (13 TP, 1 FN findings). Both WB-DWI and WB-DWI + WB-ceMRI failed to detect a lung metastasis. The remaining three metastatic findings that were not seen with WB-DWI were in the brain. Thus, the overall SE and PPV (95 % CI) of WB-DWI in detecting metastatic findings were both equal to 0.71 (0.42–0.92), whereas SE and PPV (95 % CI) of WB-DWI + WB-ceMRI were, respectively, 0.93 (0.66–1.00) and 0.57 (0.34–0.77). The difference in the detection of metastatic findings with the two protocols was not statistically significant (McNemar's test *P* value 0.08).

Among the 63 examinations that were negative by the reference standard, there were 4 FP findings for WB-DWI, whereas WB-DWI + WB-ceMRI had 10 FP findings.

Per body region analysis

According to the reference standard, the distribution of the 14 metastatic findings by body region was as follows: three in the brain, four in the chest (Fig. 2a, b), three in the abdomen, three in subcutaneous tissues (Fig. 3a, b) and one in bone (Supplementary Table 1). There was complete agreement between the two readings in the abdomen and bones, where all metastatic findings were detected by both techniques, and in the neck and pelvis, where no metastases were found. The techniques differed in findings for the brain, chest, and subcutaneous tissues. In the brain, WB-DWI + WB-ceMRI yielded three TP, three FP, and two TN findings, which were not seen by WB-DWI. In the chest, WB-DWI + WB-ceMRI yielded one additional FP (enlarged mediastinal lymph node) as well as four TN findings (two lung inflammatory changes, one thymic hyperplasia, one hiatus hernia) not reported with WB-DWI. WB-DWI + WB-ceMRI also yielded two additional FP findings in the subcutaneous tissues (enhancing scars, one in the left scapular region, the other dorsal region). The two smallest metastases found were of 2 and 3 mm, in the brain and liver (Fig. 4a, b), respectively. No malignancies besides melanoma were found.

Per patient analysis

In the reading using WB-DWI, nine out of the 19 enrolled patients were considered to have findings suspicious for metastases, of which six proved to be TP and three FP (by patient) (Fig. 5a, b). The remaining 10 patients were all considered to have benign findings, but whereas nine were TN, one was FN. WB-DWI had an SE of 85.7 % (CI 42–100 %) and SP of 75 % (CI 43–95 %) in the diagnosis of metastases, with a PPV of 66.6 % (CI 30–93 %), NPV of 90 % (CI 56–100 %), and a DA of 79 % (CI 54–94 %) (Table 5).

In the reading using WB-DWI + WB-ceMRI, 11 patients were considered to have findings suspicious for metastases, of which seven proved to be TP and four FP (by patient) (Fig. 5c, d). The remaining eight patients were considered to have benign findings and all were TN. WB-DWI + WB-ceMRI had an SE of 100 % (CI 59–100 %) and SP of 66.6 % (CI 35–90 %) in the diagnosis of metastases, with a PPV of 63.6 % (CI 31–89 %), NPV of 100 % (CI 63–100 %), and a DA of 79 % (CI 54–94 %) (Table 5).

Discussion

In our study, all examinations were completed successfully, indicating good tolerance of the procedure. Patient compliance

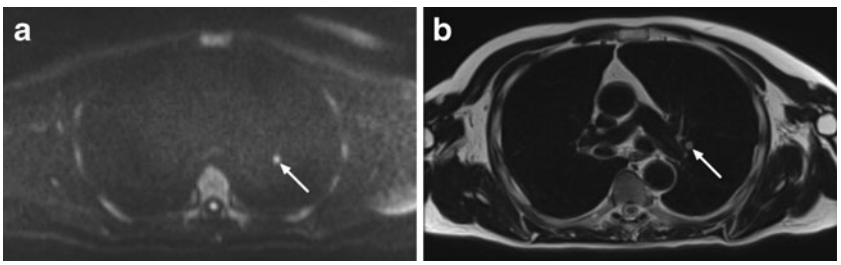

Fig. 2 A lung nodule of 6 mm in the left upper lobe in a 57-year-old man. **a** Axial WB-DWI images (b=800 s/mm^2) show a hyperintense lesion (*arrow*). **b** The T2-weighted TSE image also shows a lesion (*arrow*) adjacent to mediastinum. The lesion was considered suspicious for malignancy both using WB-DWI and WB-DWI + WB-ceMRI. The diagnosis of malignancy was confirmed by observing its increase in size in subsequent follow-up examinations

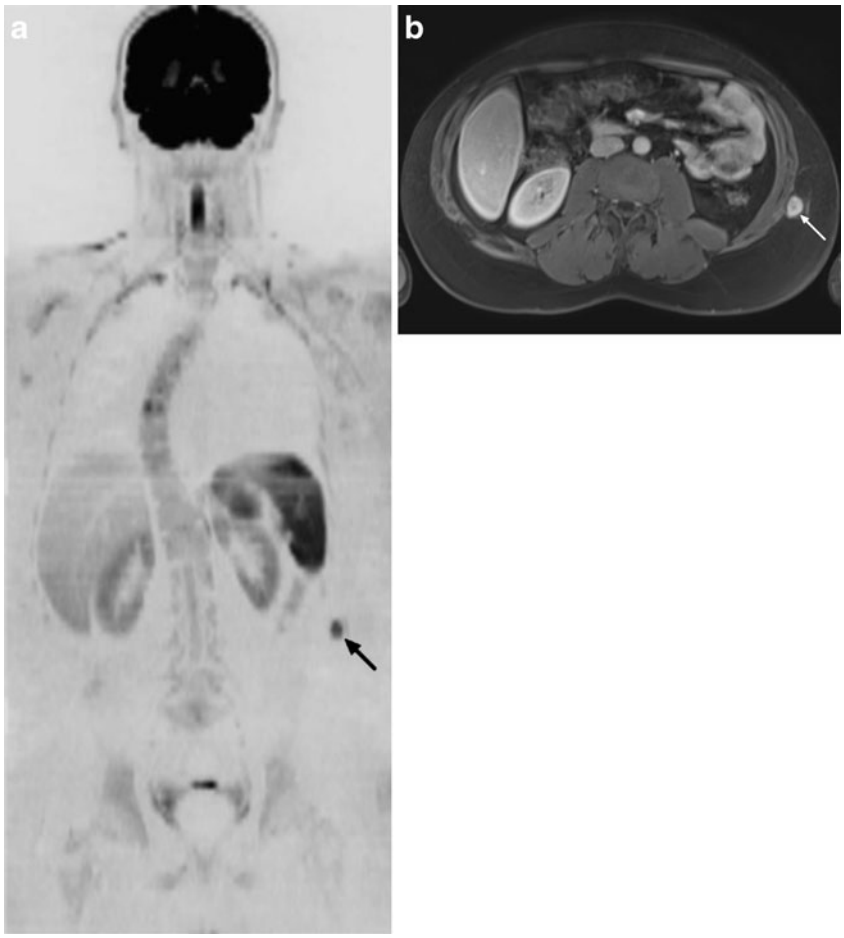

Fig. 3 A lesion of 17 mm in subcutaneous tissues in a 27-year-old man. **a** Inverted greyscale MPR of WB-DWI images (b=800 s/mm^2) show a (inverted) hyperintense lesion (*arrow*). **b** The post-contrast T1-weighted gradient echo "water" image show a contrast-enhancing lesion (*arrow*) in the subcutaneous fat of the left flank. The lesion was considered suspicious for malignancy both using WB-DWI and WB-DWI + WB-ceMRI. The diagnosis of malignancy was confirmed by ultrasound-guided biopsy

in the general population is likely to be lower as our patients were enrolled in a clinical trial, provided informed consent, and may have been motivated by their awareness of the radiation dose savings (4 mSv vs about 120 mSv per year) involved in the present study in comparison to follow-up with whole-body total-body CT.

Implications by examination

Both WB-DWI and WB-DWI + WB-ceMRI correctly identified the eight positive examinations, with very good agreement between readings (κ=85 %; 95 % CI 70–100 %) and no significant difference in their detection of metastases.

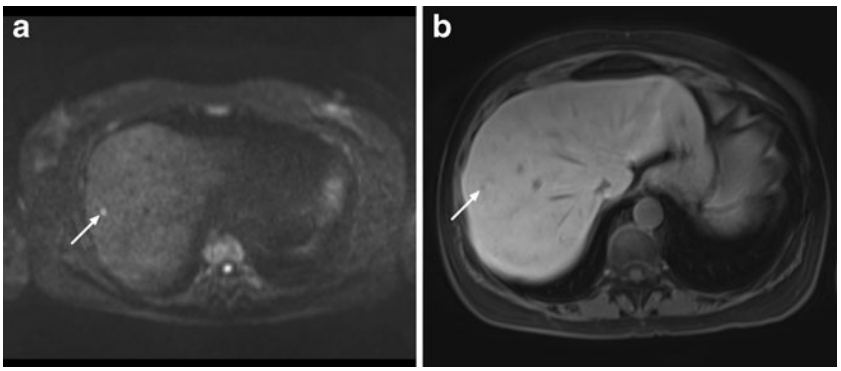

Fig. 4 A lesion of 3 mm in the liver in a 60-year-old woman. **a** Axial WB-DWI images (b=800 s/mm^2) show a hyperintense lesion in the VIII segment of the liver. **b** The post-contrast T1-weighted gradient echo "water" image performed 20 min after administration of hepatobiliary-specific agent) shows a hypointense lesion in the VIII segment of the liver. The lesion was considered diagnostic for malignancy both using WB-DWI and WB-DWI + WB-ceMRI. The diagnosis of malignancy was confirmed by observing an increase in size in subsequent follow-up examinations

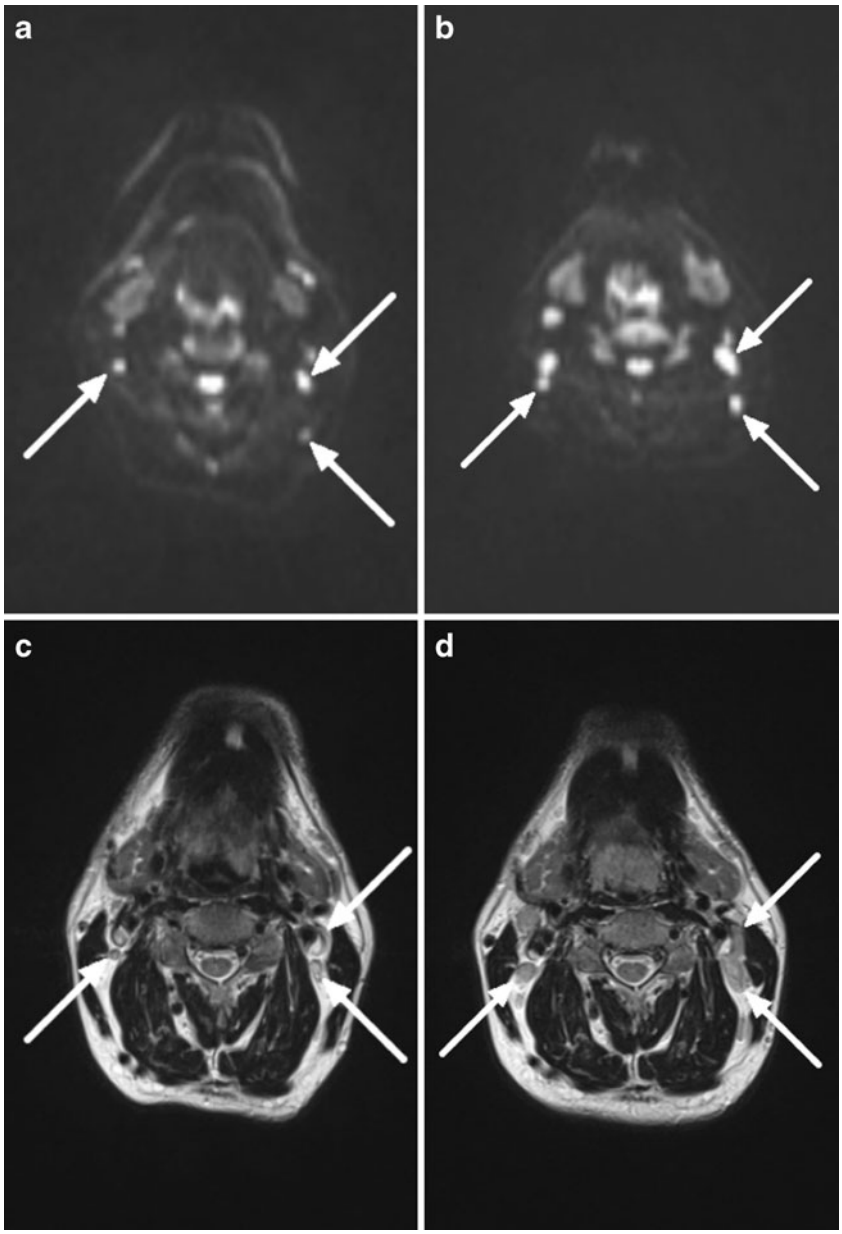

Fig. 5 False positive lymph nodes (*arrows*) in the neck in a 49-year-old man. Axial WB-DWI images (b=800 s/mm^2) obtained at baseline (**a**) and after 3 months (**b**) show increase in lymph node size as do the T2-weighted TSE obtained at baseline (**c**) and after 3 months (**d**). An increase in the size of lymph nodes was diagnosed both using WB-DWI and WB-DWI + WB-ceMRI, and therefore they were considered suspicious for malignancy. An ultrasound was therefore performed, which showed benign features. The decrease in size of these lymph nodes in the subsequent MRI examinations (not shown) confirmed their benign nature

Overall, WB-DWI demonstrated a lower SE in detection of metastases, primarily owing to its failure to detect brain metastases. In fact, limited to extracranial metastases detection, both techniques had an SE of 91 % (CI 59–100 %). Despite the lower overall SE of WB-DWI, its PPV was higher than WB-DWI + WB-ceMRI owing to the

Table 5 Findings, diagnostic accuracy, sensitivity, specificity and predictive values per patient

Reading	True positive (TP)	False positive (FP)	True negative (TN)	False negative (FN)	Diagnostic accuracy (DA, %) (95 % CI, %)	Sensitivity (SE, %)	Specificity (SP, %)	Positive predictive value (PPV, %)	Negative predictive value (NPV, %)
WB-DWI	6	3	9	1	79	85.7	75	66.6	90
					54–94	42–100	43–95	30–93	56–100
WB-DWI + WB-MRI	7	4	8	0	79	100	66.6	63.6	100
					54–94	59–100	35–90	31–89	63–100

additional false positive findings obtained with the latter (four FP using WB-DWI, and ten FP using WB-DWI + WB-ceMRI).

As WB-DWI + WB-ceMRI did not show additional metastatic findings compared to WB-DWI in neck, abdomen, pelvis, bones, and subcutaneous tissues, our results support the argument that WB-DWI alone can be considered for examination of these body regions in this clinical setting, with substantial savings in MRI time. A tailored melanoma metastases protocol consisting of extracranial WB-DWI and intracranial pre- and post-contrast T1-weighted sequences would require less than 15 min of MRI time as opposed to the 38 min 21 s of the combined WB-DWI + WB-ceMRI protocol used here, but would be expected to have identical diagnostic performance.

Implications by body region

In the brain, WB-DWI did not detect the presence of brain metastases in three cases, involving lesions of between 2 and 5 mm in diameter that were seen using WB-DWI + WB-ceMRI. WB-DWI + WB-ceMRI was, however, prone to FP findings (three out of a total of eight). The first of these results suggests that the short interval (3 months) of WB-DWI MRI did not play a role in the detection of brain metastases. The brain FP findings appear to have been sites of transient enhancement not seen on subsequent follow-up, but we are unable to attribute this observation to the therapy being administered or to other causes. The design of the study, involving frequent examinations with the aim of detecting small, asymptomatic metastases, may be expected to result in an increase of FN and FP findings. Our observations are therefore specific for our cohort and may not apply to clinical routine.

In the neck, both WB-DWI and WB-DWI + WB-ceMRI had FP findings due to benign lymph nodes that were judged suspicious because of their size. As it has been demonstrated that patients receiving ipilimumab, which acts on T-lymphocytes, may experience a reaction in benign lymph nodes, the enlarged lymph nodes may have been a treatment-specific response in patients randomized to the therapy arm of this clinical trial [21, 22]. Supporting this hypothesis, one of the two patients with an FP finding in neck lymph nodes was confirmed to be receiving ipilimumab (study blinding was broken because of acute toxicity). Although not on the market at this time, ultrasmall paramagnetic iron oxide (USPIO) contrast agents, owing to their uptake in reactive lymph nodes [23, 24], may contribute to lymph node assessment in patients undergoing anti-CTLA-4 treatment.

In the chest, WB-DWI and WB-DWI + WB-ceMRI readings again yielded FP findings attributable to enlarged lymph nodes, and one FN finding where both missed lung metastases that were no larger than 4 mm. This FN finding suggests that improvement is still needed before WB-DWI or WB-DWI + WB-ceMRI can be used as an alternative to CT in routine clinical assessment of the lungs. The implications for patient care of detecting such small lung metastases may differ according to the specific clinical setting.

Our results for the abdomen, being equivalent for both methods, suggest that WB-ceMRI made no diagnostic contribution in our cohort. As the one FP abdominal finding in our study was outside the liver, we considered our performance for the liver to be comparable to studies that have focused specifically on liver findings, where DA values up to 100 % have been reported [25, 26]. We note that we used a hepatobiliary-specific contrast agent in order to obtain the highest possible diagnostic performance in the liver, which is a possible site of metastases in melanoma patients. Although we know of no published reports on the use of Gd-EOB-DTPA in evaluating extra-hepatic metastases, this contrast agent has almost twice the T1 relaxivity of other agents, and comparative studies have demonstrated that this has advantages in terms of enhanced image contrast, image quality, and diagnostic confidence. These considerations suggest that the use of Gd-EOB-DTPA would not compromise evaluation of extra-hepatic metastases [27].

As a result of the lack of pelvic metastases in our cohort, our results cannot be considered representative of the likely performance of WB-DWI for pelvic metastases, though it has shown potential for DWI in the assessment of pelvic malignancies [28–30].

For the detection of metastases in subcutaneous tissues, WB-DWI and WB-DWI + WB-ceMRI differed only in that WB-DWI + WB-ceMRI found two fewer FP findings (both associated with scarring). This differs somewhat from the only prior study comparing WB-DWI with a WB-ceMRI protocol for the assessment of melanoma, where WB-DWI allowed the detection of more metastases in subcutaneous tissues [31].

For the evaluation of bony structures in our study, WB-ceMRI did not add to the diagnostic performance of WB-DWI. It is necessary to emphasize that these results are specific to the context of the present study where bones were assessed only for the presence of metastases, a role in which WB-DWI has shown good results [32, 33].

Implications for patients

The CIs of DA, SE, SP, PPV, and NPV for the detection of metastases at the patient level are rather broad because of the small number of patients enrolled in the study. This limits the possibilities for effective comparison between the two techniques and with other studies. Nonetheless, we can consider the DA (79 %) of both WB-DWI and WB-DWI + WB-ceMRI in our study to have been slightly lower than that in other studies where WB-ceMRI has been used for early detection of metastases, and DA values of 92 % [34] and 93 % [35, 36] reported for the correct assessment of M stage. The moderate DA

observed in our study was primarily due to the relatively high number of false findings at a patient level (three FP and one FN for WB-DWI, and four FP for WB-DWI + WB-ceMRI).

The foremost limitation of this study is the small number of patients, which limited the incidence of findings in all body regions, thus rendering the statistical analysis of the results and their clinical significance rather coarse. In part, this is compensated by repeated examinations in the same patients that allow each patient to serve as their own control. Further, except for the lung, the findings of WB-ceMRI and of WB-DWI + WB-ceMRI were not compared to established whole-body imaging techniques, such as CT and PET/CT. Our results may consequently be biased as the confirmatory investigations were only performed for findings judged suspicious on WB-DWI or WB-DWI + WB-ceMRI. Moreover, the small study size, and lack of comparison with CT or PET/CT precludes us from commenting on the clinical value of WB-DWI with or without WB-ceMRI for follow-up melanoma patients. We used a comprehensive protocol for WB-ceMRI, from head to pelvis in order to minimize any failure to identify metastases, though this led to a relatively long exam duration. There also still remains the need to validate the use of WB-DWI for metastasis detection in comparison with CT or PET/CT as the reference standard. An important implication of our results is that the potential exists for reducing MR examination times in such a study by avoiding unnecessary MR sequences.

In conclusion, whole-body diffusion-weighted imaging without additional WB-ceMRI sequences is promising for the detection of extracranial metastases, including lung metastases greater than 5 mm and even smaller metastases in the abdomen, pelvis, bones, and subcutaneous tissues. Contrast-enhanced MRI is required for evaluating the brain.

Acknowledgements We thank Guarniflon S.p.A. for the financial support of Dr. Alessi. Funding sources had no influence in acquisition, analysis, or interpretation of the data.

References

1. Forschner A, Eigentler TK, Pflugfelder A et al (2010) Melanoma staging: facts and controversies. Clin Dermatol 28:275–280
2. Siegel R, Naishadham D, Jemal A (2013) Cancer statistics, 2013. CA Cancer J Clin 63:11–30
3. Balch CM, Gershenwald JE, Soong SJ et al (2009) Final version of 2009 AJCC melanoma staging and classification. J Clin Oncol 27:6199–6206
4. Eigentler TK, Caroli UM, Radny P et al (2003) Palliative therapy of disseminated malignant melanoma: a systematic review of 41 randomised clinical trials. Lancet Oncol 4:748–759
5. Brand CU, Ellwanger U, Stroebel W et al (1997) Prolonged survival of 2 years or longer for patients with disseminated melanoma. An analysis of related prognostic factors. Cancer 79:2345–2353
6. Wong SL, Coit DG (2006) Role of surgery in patients with stage IV melanoma. Curr Opin Oncol 16:155–160
7. Sharpless SM, Das Gupta TK (1998) Surgery for metastatic melanoma. Semin Surg Oncol 14:311–318
8. Garbe C, Schaudendorf D, Regent D et al (2008) Short German guidelines: malignant melanoma. J Dtsch Dermatol Ges 6:S9–S14
9. Mayerhoefer ME, Prosch H, Herold CJ, Weber M, Karanikas G (2012) Assessment of pulmonary melanoma metastases with 18F-FDG PET/CT: which PET-negative patients require additional tests for definitive staging? Eur Radiol 22:2451–2457
10. Bafounta ML, Beauchet A, Chagnon S et al (2004) Ultrasonography or palpation for detection of melanoma nodal invasion: a meta-analysis. Lancet Oncol 5:673–680
11. Kaufmann PM, Crone-Münzebrock W (1992) Tumor follow-up using sonography and computed tomography in the abdominal region of patients with malignant melanoma. Aktuelle Radiol 2:81–85
12. Müller-Horvat C, Radny P, Eigentler TK et al (2006) Prospective comparison of the impact on treatment decisions of whole-body magnetic resonance imaging and computed tomography in patients with metastatic malignant melanoma. Eur J Cancer 42:342–350
13. Hausmann D, Jochum S, Utikal J, Hoffmann RC et al (2011) Comparison of the diagnostic accuracy of whole-body MRI and whole-body CT in stage III/IV malignant melanoma. J Dtsch Dermatol Ges 9:212–222
14. Dellestable P, Granel-Brocard F, Rat AC, Olivier P, Régent D, Schmutz JL (2011) Impact of whole body magnetic resonance imaging (MRI) in the management of melanoma patients, in comparison with positron emission tomography/computed tomography (PET/CT) and CT. Ann Dermatol Venereol 138:377–383
15. Fischer MA, Nanz D, Hany T et al (2013) Diagnostic accuracy of whole-body MRI/DWI image fusion for detection of malignant tumours: a comparison with PET/CT. Eur Radiol 21:246–255
16. Hegenscheid K, Seipel R, Schmidt CO et al (2013) Potentially relevant incidental findings on research whole-body MRI in the general adult population: frequencies and management. Eur Radiol 23:816–826
17. Platzek I, Zastrow S, Deppe PE et al (2010) Whole-body MRI in follow-up of patients with renal cell carcinoma. Acta Radiol 51:581–589
18. Pearce T, Philip S, Brown J et al (2012) Bone metastases from prostate, breast and multiple myeloma: differences in lesion conspicuity at short-tau inversion recovery and diffusion-weighted MRI. Br J Radiol 85:1102–1106
19. Takahara T, Imai Y, Yamashita T et al (2006) Diffusion weighted whole body imaging with background body signal suppression (DWIBS): technical improvement using free breathing, STIR and high resolution 3D display. Radiat Med 22:275–282
20. Kwee TC, Takahara T, Ochiai R, Nievelstein RA, Luijten PR (2008) Diffusion-weighted whole-body imaging with background body signal suppression (DWIBS): features and potential applications in oncology. Eur Radiol 18:1937–1952
21. Wolchok JD, Hoos A, O'Day S et al (2009) Guidelines for the evaluation of immune therapy activity in solid tumors: immune-related response criteria. Clin Cancer Res 15:7412–7420
22. O'Regan KN, Jagannathan JP, Ramaiya N et al (2011) Radiologic aspects of immune-related tumor response criteria and patterns of immune-related adverse events in patients undergoing ipilimumab therapy. AJR Am J Roentgenol 197:W241–W246
23. Harisinghani MG, Barentsz J, Hahn PF et al (2003) Noninvasive detection of clinically occult lymph-node metastases in prostate cancer. N Engl J Med 348:2491–2499
24. Triantafyllou M, Studer UE, Birkhäuser FD et al (2013) Ultrasmall superparamagnetic particles of iron oxide allow for the detection of metastases in normal sized pelvic lymph nodes of patients with bladder and/or prostate cancer. Eur J Cancer 49:616–624
25. Pfannenberg C, Aschoff P, Schanz S et al (2007) Prospective comparison of 18F-fluorodeoxyglucose positron emission tomography/computed tomography and whole-body magnetic resonance imaging in staging of advanced malignant melanoma. Eur J Cancer 43:557–564

26. Koh DM, Brown G, Riddell AM et al (2008) Detection of colorectal hepatic metastases using MnDPDP MR imaging and diffusion-weighted imaging (DWI) alone and in combination. Eur Radiol 18:903–910
27. Giesel FL, Mehndiratta A, Essig M (2010) High-relaxivity contrast-enhanced magnetic resonance neuroimaging: a review. Eur Radiol 10:2461–2474
28. Kim SH, Lee JY, Lee JM, Han JK, Choi BI (2011) Apparent diffusion coefficient for evaluating tumour response to neoadjuvant chemoradiation therapy for locally advanced rectal cancer. Eur Radiol 21:987–995
29. Thoeny HC, Forstner R, De Keyzer F (2012) Genitourinary applications of diffusion-weighted MR imaging in the pelvis. Radiology 263:326–342
30. Giannarini G, Petralia G, Thoeny HC (2012) Potential and limitations of diffusion-weighted magnetic resonance imaging in kidney, prostate, and bladder cancer including pelvic lymph node staging: a critical analysis of the literature. Eur Urol 61:326–340
31. Laurent V, Trausch G, Bruot O et al (2010) Comparative study of two whole-body imaging techniques in the case of melanoma metastases: advantages of multi-contrast MRI examination including a diffusion-weighted sequence in comparison with PET-CT. Eur J Radiol 75:376–383
32. Padhani AR, Koh DM, Collins DJ (2011) Whole-body diffusion-weighted MR imaging in cancer: current status and research directions. Radiology 261:700–718
33. Padhani AR, Gogbashian A (2011) Bony metastases: assessing response to therapy with whole-body diffusion MRI. Cancer Imaging 11:S129–S145
34. Schmidt GP, Baur-Melnyk A, Herzog P et al (2005) High-resolution whole-body MRI tumor staging with the use of parallel imaging versus dual modality PET-CT: experience on a 32-channel system. Invest Radiol 40:743–753
35. Antoch G, Vogt FM, Freudenberg LS et al (2003) Whole-body dual-modality PET/CT and whole-body MRI for tumor staging in oncology. JAMA 290:3199–3206
36. Layer G, Steudel A, Schuller H et al (1999) Magnetic resonance imaging to detect bone marrow metastases in the initial staging of small cell lung carcinoma and breast carcinoma. Cancer 85:1004–1009